

Figure 3. Same plot as in Figure 2, but for $E_s = 0.8$ eV. Other parameters as in Figures 1 and 2.

myoglobins,^{30,31} while Figure 3 corresponds to a somewhat smaller reorganization free energy.

(2) Inclusion of the modulation effects also shifts the whole free energy plot horizontally toward lower values without significant changes of its shape (Figures 2 and 3). For the data in ref 31 ($R = 12$ Å), the shift would amount to 0.15–0.20 eV but

would be expected to be larger for free energy relations based on substitution at more remote sites from the heme group.

Free energy relations based on Ru modification at different histidines might offer a new perspective also for illumination of environmental modulation of the electronic factor in electron-transfer theory. At the same time the continuum formalism used,^{24–26} which can be extended to solvent structural effects in the form of vibrational and spatial dielectric dispersion, is a useful frame for incorporation of large numbers of solvent molecules and nonequilibrium solvation effects for which quantum chemical approaches are not feasible. On the basis of this formalism, a family of almost parallel free energy plots would be expected when the Ru fragments are attached to different His sites. These plots are shifted to lower reaction free energies with increasing electron-transfer distance, and the equilibrium values of the electronic parameters can, in principle, be extracted from the shifts.

Acknowledgment. We thank Julie Damms Studiefond and Otto Mønstedts Fond for financial support.

Structure and Reactivity of Titanium/Platinum and Palladium Heterobinuclear Complexes with μ -Methylene Ligands

Fumiyuki Ozawa, Joon Won Park, Peter B. Mackenzie, William P. Schaefer, Lawrence M. Henling, and Robert H. Grubbs*

Contribution No. 7821 from the Arnold and Mabel Beckman Laboratories of Chemical Synthesis, California Institute of Technology, Pasadena, California 91125. Received July 28, 1988

Abstract: A series of titanium/platinum and palladium heterobinuclear μ -methylene complexes $\text{Cp}_2\text{TiCH}_2\text{MX}(\text{Me})\text{L}$ has been prepared: $\text{M} = \text{Pt}$, $\text{X} = \text{Cl}$, $\text{L} = \text{PMe}_3$ (**2b**), PMe_2Ph (**2c**), PMePh_2 (**2d**); $\text{M} = \text{Pt}$, $\text{X} = \text{Me}$, $\text{L} = \text{PMe}_2\text{Ph}$ (**2e**, **2f**); $\text{M} = \text{Pd}$, $\text{X} = \text{Cl}$, $\text{L} = \text{PMe}_3$ (**2g**). The $\mu\text{-CH}_2/\mu\text{-Cl}$ complex **2c** crystallizes in the monoclinic system in space group $P2_1/n$ (No. 14), with $a = 13.249$ (3) Å, $b = 11.646$ (3) Å, $c = 14.542$ (5) Å, $\beta = 114.45$ (2)°, $V = 2042.6$ (10) Å³, $Z = 4$, and density = 1.87 g cm⁻³. The $\mu\text{-CH}_2/\mu\text{-CH}_3$ analogue **2e** is isostructural to **2c** and also crystallizes in space group $P2_1/n$ (No. 14) with $a = 13.333$ (4) Å, $b = 11.686$ (2) Å, $c = 14.351$ (2) Å, $\beta = 115.03$ (2)°, $V = 2026.0$ (8) Å³, $Z = 4$, and density = 1.82 g cm⁻³. Structural studies indicate the following: (1) the Ti-CH₂ bond possesses residual double-bond character, (2) there is a dative Pt \rightarrow Ti interaction, which may be regarded as π back-donation from the platinum atom to the "Ti=CH₂" group, and (3) the $\mu\text{-CH}_3$ group in **2e** is bound to the titanium atom through a three-center, two-electron agostic bond. Complexes **2c** and **2d** react with tertiary phosphines to give $\text{Cp}_2(\text{Cl})\text{TiCH}_2\text{Pt}(\text{Me})\text{L}_2$ species, which form $\mu\text{-(C,O)}$ -ketene complexes $\text{Cp}_2(\text{Cl})\text{TiOC(=CH}_2\text{)Pt}(\text{Me})\text{L}_2$ upon carbonylation. The palladium complex **2g** undergoes a reductive elimination reaction to give $\text{Cp}_2\text{Ti}(\text{Et})\text{Cl}$ and Pd^0PMe_3 complexes.

Recently much attention has been focused upon early-transition-metal/late-transition-metal heterobinuclear complexes¹ because of their potential applications in catalytic organic reactions. Also, these complexes have been studied in order to gain an

understanding of the phenomenon of so-called "strong metal-support interactions (SMSI)" in heterogeneous catalysis.² It is well documented that late transition metals, which are finely dispersed on early-transition-metal oxide supports such as TiO₂ and ZrO₂, serve as highly active catalysts in the catalytic hydrogenation of carbon monoxide. SMSI have been observed in such systems. While the exact nature of the interaction is still unclear, SMSI are regarded as the prime reason for the enhanced catalytic activity.³

(1) (a) Jacobsen, E. N.; Goldberg, K. I.; Bergman, R. G. *J. Am. Chem. Soc.* **1988**, *110*, 3706. (b) White, G. S.; Stephan, D. W. *Organometallics* **1988**, *7*, 903. (c) Gelmini, L.; Stephan, D. W. *Ibid.* **1988**, *7*, 849. (d) White, G. S.; Stephan, D. W. *Ibid.* **1987**, *6*, 2169, and references cited therein. (e) Sartain, W. J.; Selegue, J. P. *Organometallics* **1987**, *6*, 1812; *J. Am. Chem. Soc.* **1985**, *107*, 5818. (f) Casey, C. P.; Jordan, R. F.; Rheingold, A. L. *J. Am. Chem. Soc.* **1983**, *105*, 665, and references cited therein. (g) Casey, C. P.; Palermo, R. E.; Rheingold, A. L. *Ibid.* **1986**, *108*, 549. (h) Casey, C. P.; Palermo, R. E.; Jordan, R. F.; Rheingold, A. L. *Ibid.* **1985**, *107*, 4597. (i) Casey, C. P.; Jordan, R. F.; Rheingold, A. L. *Organometallics* **1984**, *3*, 504. (j) Casey, C. P.; Nief, F. *Ibid.* **1985**, *4*, 1218. (k) Barger, P. T.; Bercaw, J. E. *Ibid.* **1984**, *3*, 278. (l) Choukroun, R.; Gervais, D.; Jaud, J.; Kalck, P.; Senocq, F. *Ibid.* **1986**, *5*, 67. (m) Ferguson, G. S.; Wolczanski, P. T. *Ibid.* **1985**, *4*, 1601. (n) Tso, C. T.; Cutler, A. R. *J. Am. Chem. Soc.* **1986**, *108*, 6069. (o) Ortiz, J. V. *Ibid.* **1986**, *108*, 550. (p) Sternal, R. S.; Sabat, M.; Marks, T. J. *Ibid.* **1987**, *109*, 7920. (q) Sternal, R. S.; Marks, T. J. *Organometallics* **1987**, *6*, 2621. (r) Bullock, R. M.; Casey, C. P. *Acc. Chem. Res.* **1987**, *20*, 167.

(2) (a) Baker, R. T. K.; Tauster, S. J.; Dumesic, J. A., Eds. *Strong Metal-Support Interactions*; American Chemical Society: Washington, DC 1986. (b) Imelik, B.; Naccache, C.; Coudurier, G.; Praliaud, H.; Meriaudeau, P.; Gallezot, P.; Martin, G. A.; Verdrine, J. C., Eds. *Metal-Support and Metal-Additive Effects in Catalysis*; Elsevier: New York, 1982.

(3) For recent examples, see: (a) Mori, T.; Masuda, H.; Imai, H.; Taniguchi, S.; Miyamoto, A.; Hattori, T.; Murakami, Y. *J. Chem. Soc., Chem. Commun.* **1986**, 1244. (b) Iwasawa, Y.; Sato, H. *Chem. Lett.* **1985**, 507. (c) Doi, Y.; Miyake, H.; Soga, K. *J. Chem. Soc., Chem. Commun.* **1987**, 347. (d) Rieck, J. C.; Bell, A. T. *J. Catal.* **1986**, *99*, 262. (e) Vannice, M. A.; Twu, C. C. *Ibid.* **1983**, *82*, 213. (f) Vannice, M. A.; Sudhakar, C. *J. Phys. Chem.* **1984**, *88*, 2429.

Table I. NMR Data for the μ -Methylene Complexes

complex				¹ H NMR			¹³ C{ ¹ H} NMR				³¹ P{ ¹ H} NMR			
X	Y	Z	M	δ	<i>J</i> , Hz		δ	<i>J</i> , Hz		[<i>J</i> _{CH}], Hz	assignments	δ^b	¹ <i>J</i> _{PtP} , Hz	
Cl	Me (2b)	PMe ₃	Pt	8.00 (d)	5.2	38.6	180.5 (d)	59	396	135	μ -CH ₂	-20.2	2730	
				5.52 (d)	0.0	0.0	107.9 (s)	0	0	172	Cp			
				1.13 (d)	9.3	27.6	15.2 (d)	31	37	129	PMe			
				0.88 (d)	8.5	94.2	-15.7 (d)	5	824	130	PtMe			
Cl	Me (2c)	PMe ₂ Ph	Pt	8.09 (d)	5.1	39.3	179.2 (d)	58	409	136	μ -CH ₂	-8.1	2788	
				5.57 (s)	0.0	0.0	108.1 (s)	0	0	174	Cp			
				1.51 (d)	9.0	26.9	14.9 (d)	31	34	129	PMe			
				1.01 (d)	8.5	93.8	-14.4 (d)	5	822	130	PtMe			
Cl	Me (2d)	PMePh ₂	Pt	7.95 (d)	5.4	39.8	177.5 (d)	70	419	135	μ -CH ₂	7.3	2803	
				5.52 (s)	0.0	0.0	108.1 (s)	0	0	173	Cp			
				1.93 (d)	8.5	26.1	14.9 (d)	31	31	131	PMe			
				0.86 (d)	8.3	93.8	-12.7 (d)	5	821	130	PtMe			
Me	Me (2e)	PMe ₂ Ph	Pt	7.92 (d)	4.4	33.5	178.5 (d)	66	472	137	μ -CH ₂	-2.8	2450	
				5.28 (s)	0.0	0.0	105.1 (s)	0	0	173	Cp			
				1.44 (d)	8.3	23.7	13.8 (d)	30	30	129	PMe			
				0.72 (d)	8.8	64.7	-10.1 (d)	8	565	125	PtMe			
				~-3 (br)	<i>c</i>	<i>c</i>	47.6 (s)	0	381	115 ^d	μ -Me (at rt)			
				1.20 (d)							μ -Me (at -82 °C)			
				-12.4 (t)										
Me	PMe ₂ Ph (2f)	Me	Pt	7.42 (d)	6.0	22.5	180.0 (d)	5	324	133	μ -CH ₂	-3.5	2690	
				5.22 (s)	0.0	0.0	105.0 (s)	0	0	173	Cp			
				1.45 (d)	8.8	25.9	14.2 (d)	34	34	129	PMe			
				0.82 (d)	7.8	59.6	-10.6 (d)	9	540	125	PtMe			
				~-3 (br)	<i>c</i>	<i>c</i>	46.9 (d)	88	553	120 ^d	μ -Me (at rt)			
				1.61 (d)							μ -Me (at -82 °C)			
				-11.3 (t)										
Cl	Me (2g) (at -20 °C)	PMe ₃	Pd	8.26 (d)	4.6		191.3 (d)	51		132	μ -CH ₂	-17.6		
				5.51 (s)	0.0		107.8 (s)	0		174	Cp			
				0.96 (d)	8.6		15.2 (d)	23		129	PMe			
				0.80 (d)	8.3		-1.1 (d)	7		132	PdMe			
				(nonagostic μ -CH ₃)							² <i>J</i> _{HH} = 12.5 Hz			
				(agostic μ -CH ₃)										
				(nonagostic μ -CH ₃)								² <i>J</i> _{HH} = 12.8 Hz		
				(agostic μ -CH ₃)										

^aAll data are recorded at room temperature unless otherwise noted. Solvent: benzene-*d*₆ (2c, 2e, 2f), toluene-*d*₈ (2b, 2d, 2g), toluene-*d*₈/THF-*d*₈ = 3/1 (2e, 2f at -82 °C). ^bChemical shift is referred to an external 85% H₃PO₄ standard (downfield positive). ^cCoupling constant is obscure due to broadening. ^dSee ref 5c.

Key intermediates in heterogeneous CO hydrogenation are μ -methylene species.⁴ We recently developed a convenient synthetic route to titanium/late-transition-metal μ -methylene complexes. These complexes serve as possible models for surface methylene species on catalysts that exhibit the SMSI phenomenon.⁵ Reactions of the "Cp₂Ti=CH₂" species generated from bis(cyclopentadienyl)titanacyclobutanes or Tebbe's reagent with late-transition-metal chlorides (L_nMCl) give a new class of μ -methylene complexes Cp₂TiCH₂M(Cl)L_n (2).^{5b} Anion exchange of the μ -Cl ligand in 2 with MeMgBr or MeLi forms μ -CH₂/ μ -CH₃ complexes.^{5c} These methods have enabled us to study a wide variety of early/late heterobinuclear complexes with μ -methylene ligands.

In this paper we describe the structure and reactivity of titanium/platinum and palladium μ -methylene complexes Cp₂TiCH₂MX(Me)L (M = Pt, Pd; X = Cl, Me; L = tertiary phosphine ligands). X-ray diffraction studies on the platinum

compounds have suggested that the Ti-CH₂ bond is intermediate in character between a single and a double bond, while the Pt-CH₂ bond exhibits both σ - and π -bonding properties. These bonding features are demonstrated in the reactions of these complexes with tertiary phosphines. The μ -methylene complexes react in the manner expected for surface methylene species in CO-hydrogenation systems. Thus, the platinum μ -CH₂/ μ -Cl complexes represent the first example of carbonylation of a μ -methylene species to afford a μ -(C,O)-ketene complex.⁶ The Ti/Pd complex undergoes a coupling reaction between the terminal methyl and μ -methylene ligands. This type of reaction is assumed to initiate chain growth in the Fischer-Tropsch reaction.⁷

Results

Synthesis of μ -Methylene Complexes. The μ -methylene complexes prepared in this study are listed in Table I. Reaction of bis(cyclopentadienyl)titanacyclobutane (1) with PtMeCl(SMe₂)₂ in toluene affords a μ -methylene/ μ -chloride complex with a SMe₂

(4) (a) Herrmann, W. A. *Adv. Organomet. Chem.* **1982**, *20*, 159. (b) Masters, C. *Ibid.* **1979**, *19*, 63. (c) Herrmann, W. A. *Angew. Chem., Int. Ed. Engl.* **1982**, *21*, 117. (d) Holton, J.; Lappert, M. F.; Pearce, R.; Yarrow, P. I. *W. Chem. Rev.* **1983**, *83*, 135. (e) Casey, C. P.; Audett, J. D. *Ibid.* **1986**, *86*, 339. (f) Muetterties, E. L. *Ibid.* **1982**, *11*, 283.

(5) (a) Mackenzie, P. B.; Ott, K. C.; Grubbs, R. H. *Pure Appl. Chem.* **1984**, *56*, 59. (b) Mackenzie, P. B.; Coots, R. J.; Grubbs, R. H., submitted to publication. (c) Park, J. W.; Mackenzie, P. B.; Schaefer, W. P.; Grubbs, R. H. *J. Am. Chem. Soc.* **1986**, *108*, 6402.

(6) (a) Geoffroy, G. L.; Bassner, S. L. *Adv. Organomet. Chem.* **1988**, *28*, 1. (b) Morrison, E. D.; Steinmetz, G. R.; Geoffroy, G. L.; Fultz, W. C.; Rheingold, A. L. *J. Am. Chem. Soc.* **1983**, *105*, 4104; **1984**, *106*, 4783. (c) Morrison, E. D.; Geoffroy, G. L.; Rheingold, A. L. *Ibid.* **1985**, *107*, 254; **1985**, *107*, 3541. (d) Lin, Y. C.; Calabrese, J. C.; Wreford, S. S. *Ibid.* **1983**, *105*, 1679. See also ref 5a.

(7) Brady, R. C.; Pettit, R. *J. Am. Chem. Soc.* **1980**, *102*, 6181; **1981**, *103*, 1287.

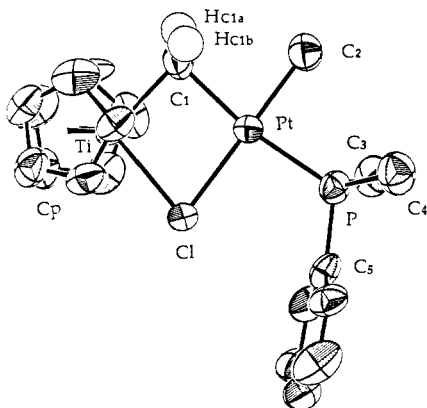
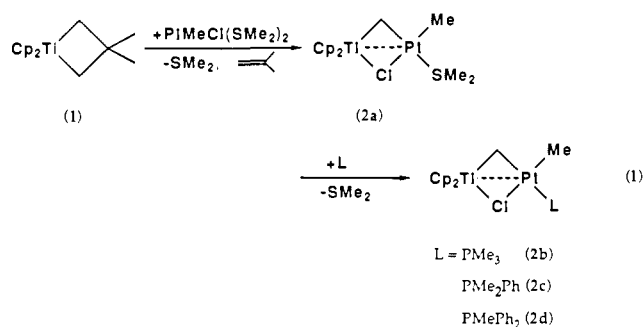


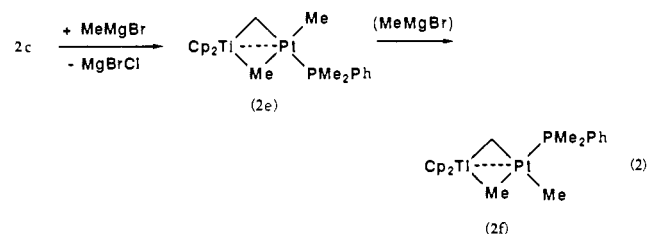
Figure 1. ORTEP diagram of complex **2c**. The ellipsoids are drawn at the 50% probability level except for the hydrogen atoms. The hydrogen atoms of the cyclopentadienyl, terminal methyl, and PMe_2Ph ligands are omitted for clarity.

ligand (**2a**) along with the evolution of a quantitative amount of isobutylene.^{5b}



Treatment of **2a** with tertiary phosphines at room temperature gives phosphine-coordinated complexes **2b–2d** in quantitative yields as confirmed by NMR spectroscopy. The palladium analogue **2g** is prepared by reaction of **1** with $[\text{PdMe}(\mu\text{-Cl})\text{PMe}_3]_2$. Compounds **2c**, **2d**, and **2g** have been isolated as red crystals and **2b** as a spectroscopically pure, oily material.

The bridging chloride ligand in **2c** is readily replaced by the methyl group of MeMgBr at room temperature to give the $\mu\text{-CH}_2/\mu\text{-CH}_3$ complex **2e**, which has been isolated as reddish orange



crystals. This reaction proceeds with retention of the original configuration about the platinum center, while on prolonged reaction **2e** is isomerized to its geometrical isomer **2f**. The isomerization is a significantly slower process in the absence of MeMgBr , suggesting a MeMgBr -promoted isomerization reaction.⁸

NMR Data. The ^1H and ^{13}C NMR resonances for the $\mu\text{-CH}_2$ group appear in the typical regions reported for binuclear μ -methylene complexes (Table I).^{4a} The $^1J_{\text{CH}}$ values are in the range of 135 ± 3 Hz; the values are intermediate between those for pure sp^2 and sp^3 carbons.⁹ The geometries at platinum and palladium in the phosphine-coordinated complexes have been determined on the basis of coupling constants between phosphorus and carbons

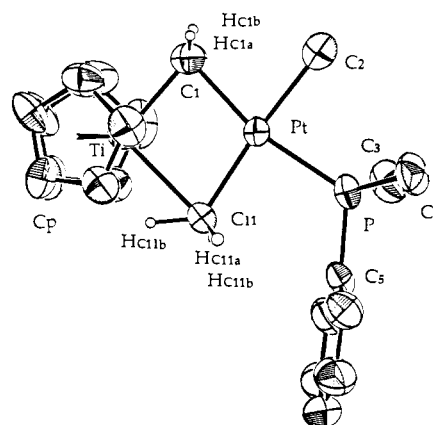


Figure 2. ORTEP diagram of complex **2e**. The ellipsoids are drawn at the 50% probability level except for the hydrogen atoms. The hydrogen atoms of the cyclopentadienyl, terminal methyl, and PMe_2Ph ligands are omitted for clarity.

Table II. Crystal and Intensity Collection Data

Complex 2c	
formula: $\text{C}_{20}\text{H}_{26}\text{ClPPtTi}$	formula wt: 575.84
cryst color: orange-red	habit: irregular plates
$a = 13.249$ (3) Å	$\beta = 114.45$ (2)°
$b = 11.646$ (3) Å	$Z = 4$
$c = 14.542$ Å	$T: 23$ °C
$V = 2042.6$ (10) Å ³	absences: $0k0, k$ odd;
$\lambda = 0.71073$ Å	$h0l, h + l$ odd
graphite monochromator	$\mu = 77.98$ cm ⁻¹
space gp: $P2_1/n$	($\mu_{\text{r,max}} = 1.08$)
cryst size: $0.24 \times 0.13 \times 0.04$ mm	$\theta\text{-}2\theta$ scan
	octants colld; $\pm h, \pm k, l$
CAD-4 diffractometer	
2θ range: $2\text{--}40^\circ$	
no. reflns measd: 3837	
no. of independent reflns: 1900	
no. with $F_o^2 > 0$: 1717	
no. with $F_o^2 > 3\sigma(F_o^2)$: 1233	
goodness of fit for merging data: 1.07	
final R index: 0.0621	
(0.035 for $F_o^2 > 3\sigma(F_o^2)$)	
final goodness of fit: 1.15	
Complex 2e	
formula: $\text{C}_{21}\text{H}_{29}\text{PPtTi}$	formula wt: 555.42
cryst color: orange-red	habit: prismatic
$a = 13.333$ (4) Å	$\beta = 115.03$ (2)°
$b = 11.686$ (2) Å	$Z = 4$
$c = 14.351$ (3) Å	$T: 23$ °C
$V = 2026.0$ (8) Å ³	absences: $0k0, k$ odd;
$\lambda = 0.7107$ Å	$h0l, h + l$ odd
graphite monochromator	$\mu = 77.42$ cm ⁻¹
space gp: $P2_1/n$	($\mu_{\text{r,max}} = 1.81$)
cryst size: $0.42 \times 0.14 \times 0.15$ mm	$\theta\text{-}2\theta$ scan
	octants colld; $\pm h, k, \pm l$
CAD-4 diffractometer	
2θ range: $2\text{--}50^\circ$	
no. reflns measd: 8745	
no. of independent reflns: 3540	
no. with $F_o^2 > 0$: 3308	
no. with $F_o^2 > 3\sigma(F_o^2)$: 2614	
goodness of fit for merging data: 0.99	
final R index: 0.0394	
(0.0242 for $F_o^2 > 3\sigma(F_o^2)$)	
final goodness of fit: 1.12	

bound to the metal.¹⁰ The carbon that is trans to the phosphine ligand gives relatively large $^2J_{\text{CP}}$ values (51–88 Hz), whereas carbons in cis positions show a small coupling (<10 Hz) with the phosphorus. In the ^1H NMR spectra of **2e** and **2f** at -82 °C, the

(8) (a) Ozawa, F.; Kurihara, K.; Yamamoto, T.; Yamamoto, A. *J. Organomet. Chem.* **1985**, 279, 233. (b) Ozawa, F.; Kurihara, K.; Fujimori, M.; Hidaka, T.; Toyoshima, T.; Yamamoto, A. *Organometallics*, in press.

(9) Silverstein, R. M.; Bassler, G. C.; Morrill, T. C. *Spectrometric Identification of Organic Compounds*, 4th ed.; Wiley: New York, 1981.

(10) Pregosin, P. S.; Kunz, R. W. ^{31}P and ^{13}C NMR of Transition Metal Phosphine Complexes; Springer-Verlag: Berlin, 1979.

Table III. Final Positional Parameters

atom	x	y	z	$U_{eq}^a (\times 10^4)$ or B^b	atom	x	y	z	$U_{eq}^a (\times 10^4)$ or B^b
Complex 2c									
Pt	2130 (0.5)	1353 (0.5)	60 (0.5)	446 (1)	C10	1083 (14)	-1955 (14)	506 (12)	663 (53)
Ti	2268 (2)	1594 (2)	-1912 (2)	451 (7)	Cp1	3640 (15)	2134 (20)	-2440 (16)	937 (78)
Cl	2061 (4)	-150 (3)	-1092 (3)	598 (12)	Cp2	3729 (13)	969 (15)	-2371 (13)	678 (56)
P	2203 (3)	91 (3)	1268 (3)	510 (12)	Cp3	4102 (13)	738 (15)	-1312 (15)	717 (64)
C1	2156 (13)	2736 (14)	-870 (13)	557 (50)	Cp4	4179 (13)	1766 (19)	-809 (12)	710 (63)
C2	2181 (12)	2658 (13)	1047 (11)	663 (50)	Cp5	3920 (15)	2657 (14)	-1541 (22)	960 (95)
C3	3514 (12)	165 (12)	2408 (10)	798 (60)	Cp6	748 (14)	2729 (13)	-2995 (14)	732 (65)
C4	1178 (13)	274 (12)	1777 (11)	817 (51)	Cp7	311 (13)	1811 (16)	-2663 (12)	636 (51)
C5	2112 (12)	-1440 (12)	947 (10)	521 (40)	Cp8	494 (14)	828 (13)	-3115 (13)	673 (55)
C6	3037 (12)	-2058 (14)	1028 (12)	658 (51)	Cp9	1128 (14)	1125 (15)	-3641 (11)	706 (58)
C7	2959 (15)	-3185 (15)	732 (13)	804 (65)	Cp10	1272 (14)	2301 (16)	-3568 (13)	748 (59)
C8	1923 (20)	-3658 (15)	311 (12)	854 (62)	HCl1a	2811 (86)	3273 (85)	-495 (78)	5.0 ^b
C9	983 (15)	-3084 (18)	193 (14)	957 (70)	HCl1b	1571 (101)	3070 (100)	-995 (105)	5.0 ^b
Complex 2e									
Pt	2178 (0.2)	1307 (0.2)	-4 (0.1)	396	Cp2	3707 (5)	937 (7)	-2380 (5)	663 (18)
Ti	2287 (0.7)	1541 (0.7)	-1883 (0.6)	385 (0.2)	Cp3	4103 (5)	673 (6)	-1338 (5)	609 (17)
P	2246 (1)	16 (1)	1213 (1)	454 (3)	Cp4	4219 (5)	1683 (7)	-810 (6)	716 (20)
C1	2195 (6)	2759 (5)	-832 (5)	562 (16)	Cp5	3933 (6)	2583 (7)	-1514 (8)	840 (24)
C2	2216 (5)	2580 (5)	1051 (4)	702 (16)	Cp6	751 (6)	2652 (6)	-2967 (5)	669 (19)
C3	3552 (6)	81 (8)	2367 (5)	726 (21)	Cp7	304 (5)	1746 (6)	-2618 (5)	646 (17)
C4	1214 (7)	203 (8)	1726 (6)	704 (19)	Cp8	494 (5)	738 (6)	-3012 (5)	609 (17)
C5	2128 (4)	-1509 (5)	898 (4)	460 (13)	Cp9	1072 (5)	997 (6)	-3601 (5)	605 (17)
C6	3055 (6)	-2161 (6)	1033 (5)	600 (16)	Cp10	1217 (6)	2190 (6)	-3581 (5)	654 (19)
C7	2973 (7)	-3289 (7)	758 (6)	760 (20)	HC1a	1535 (42)	3175 (41)	-1048 (37)	3.6 (12) ^b
C8	1969 (8)	-3814 (7)	314 (5)	810 (23)	HC1b	2804 (40)	3259 (41)	-460 (36)	3.5 (12) ^b
C9	1044 (8)	-3201 (7)	177 (6)	818 (24)	HC11a	2719 (47)	-503 (50)	-575 (44)	4.7 (17) ^b
C10	1102 (6)	-2056 (6)	455 (5)	634 (17)	HC11b	2233 (38)	-76 (39)	-1649 (38)	3.6 (11) ^b
C11	2156 (7)	-103 (6)	-944 (5)	541 (16)	HC11c	1482 (54)	-510 (52)	-1043 (47)	5.8 (18) ^b
Cp1	3630 (6)	2105 (8)	-2476 (7)	782 (22)					

^a $U_{eq} = \frac{1}{3} \sum_i \sum_j [U_{ij}(a_i^* a_j^*) (\bar{a}_i \bar{a}_j)]$. ^b Isotropic displacement parameter, B .

protons in the bridging methyl group are observed as two sets of signals, doublet and triplet, in a 2:1 ratio with geminal coupling between the protons, which coalesce into a broad singlet at elevated temperatures. As seen from the X-ray structure of **2e** described below, the appearance of two sets of signals at low temperature is ascribed to the presence of an agostic interaction between the methyl group and the titanium atom. A similar bonding pattern has been observed for $Cp_2TiCH_2Rh(CH_3)(COD)$ ($COD = 1,5$ -cyclooctadiene).^{5c}

X-ray Structures. Complexes **2c** and **2e** have been subjected to single-crystal X-ray diffraction studies. Details of data collection are summarized in Table II. Positional parameters for non-hydrogen atoms and refined hydrogen parameters are given in Table III. Selected bond lengths and bond angles are listed in Table IV. As seen from the ORTEP diagrams (Figures 1 and 2), both complexes have similar structures. The four central atoms—Ti, Pt, the μ -methylene carbons (C1), and the other bridging atom (Cl in **2c** or μ -methyl C11 in **2e**)—form a four-membered ring lying approximately in a plane with a methylene hydrogen and a Cp ring above and below the plane. The H—C—H angle of the μ -CH₂ group is normal for binuclear μ -methylene complexes.^{4a} The plane comprised of the methylene carbon and the two methylene hydrogens is tilted toward the platinum (Figure 3). The coordination geometry about titanium is pseudotetrahedral, whereas the platinum is basically in a square-planar environment.

Structure of 2e. The μ -methyl group forms a three-center, two-electron agostic bond with the titanium atom. The distance between titanium and the agostic hydrogen HC11b (1.93 (5) Å) is shorter than that in $Cp_2TiCH_2Rh(CH_3)(COD)$ (2.02 (6) Å), whereas the Ti—CH₂ bond (2.395 (8) Å) is longer than that in the Ti/Rh analogue (2.294 (6) Å).^{5b} The Ti—Pt distance is 2.776 (1) Å, which is short enough to form a dative Pt → Ti bond.¹ The presence of a Pt—Ti bond is reflected in the narrow Ti—C1—Pt angle (82.9 (3)°); the magnitude of this angle is typical of binuclear μ -methylene complexes with a metal—metal bond.^{4a} The Pt—CH₂ bond (2.078 (7) Å) is slightly shorter than those in bis(tertiary phosphine)platinacyclobutanes (2.13–2.15 Å).¹¹ The Pt—Me

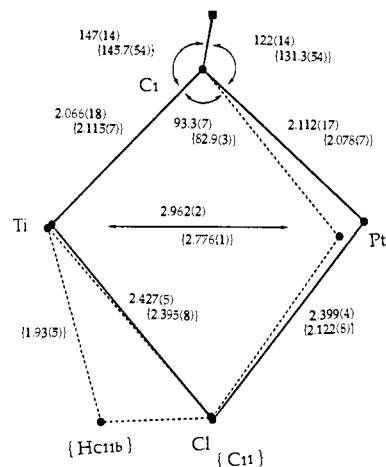


Figure 3. Comparison of the cores of complexes **2c** (—) and **2e** (---). The square mark (□) shows the intermediate point of the two μ -CH₂ hydrogens. The distances are given in angstroms and the angles in degrees. The information in brackets is for **2e**.

bridging (2.122 (8) Å) and terminal (2.108 (6) Å) bond lengths are in the typical range of a Pt—Me bond having a trans ligand with a large trans influence.¹² The Ti—CH₂ distance (2.115 (7) Å) is slightly shorter than that in $Cp_2TiCH_2C(Me)_2CH_2$ (2.16 Å)¹³ but much longer than the calculated distance for the Ti=CH₂ double bond (1.85–1.88 Å).¹⁴

(11) (a) Yarrow, D. J.; Ibers, J. A.; Lenarda, M.; Graziani, M. *J. Organomet. Chem.* **1974**, *70*, 133. (b) Rajaram, J.; Ibers, J. A. *J. Am. Chem. Soc.* **1978**, *100*, 829. (c) Lenarda, M.; Pahor, N. B.; Calligaris, M.; Graziani, M.; Randaccio, L. *J. Chem. Soc., Dalton Trans.* **1978**, 279.

(12) Wisner, J. M.; Bartczak, T. J.; Ibers, J. A.; Low, J. J.; Goddard, W. A., III *J. Am. Chem. Soc.* **1986**, *108*, 347.

(13) (a) Straus, D. A.; Grubbs, R. H. *Organometallics* **1982**, *1*, 1658. (b) Straus, D. A. Ph.D. Thesis, California Institute of Technology, Pasadena, CA, 1983.

(14) Upton, T. H.; Rappe, A. K. *J. Am. Chem. Soc.* **1985**, *107*, 1206.

Table IV. Selected Distances and Angles

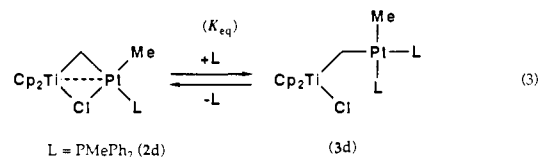
distance, Å		angle, deg	
Complex 2c			
Pt...Ti	2.962 (2)	C1-Pt-C2	83.1 (6)
Cl...C1	3.374 (18)	C1-Pt-P	170.4 (5)
Pt-Cl	2.399 (4)	C1-Pt-C1	96.6 (5)
Pt-C1	2.112 (17)	C2-Pt-P	87.7 (5)
Pt-C2	2.071 (15)	Pt-Cl-Ti	75.7 (1)
Pt-P	2.261 (4)	Cl-Ti-C1	97.0 (5)
Ti-Cl	2.427 (5)	CpC1-Ti-CpC2	132.4
Ti-C1	2.066 (18)	Ti-C1-Pt	90.3 (7)
Ti-CpC1	2.071	Pt-P-C3	113.0 (5)
Ti-CpC2	2.082	Pt-P-C4	116.3 (5)
C1-HC1a	1.03 (11)	Pt-P-C5	117.2 (5)
C1-HC1b	0.82 (14)	HC1a-C1-HC1b	110.1 (113)
P-C3	1.842 (16)		
P-C4	1.809 (16)		
P-C5	1.833 (15)		
Pt...HC1a	2.66 (11)		
Pt...HC1b	2.44 (13)		
Ti...HC1a	2.71 (11)		
Ti...HC1b	2.57 (13)		
Complex 2e			
Pt-C1	2.078 (7)	C1-Pt-C11	105.7 (3)
Pt-C11	2.122 (8)	C11-Pt-P	87.6 (2)
Pt-C2	2.108 (6)	P-Pt-C2	86.3 (2)
Pt-P	2.279 (2)	C2-Pt-C1	80.3 (3)
Pt...Ti	2.776 (1)	C1-Ti-C11	95.7 (3)
Pt...HC1a	2.58 (5)	CpA-Ti-CpB	133.3
Pt...HC1b	2.61 (5)	pt-C1-Ti	82.9 (3)
Pt...HC11a	2.48 (6)	Pt-C1-HC1a	112.1 (32)
Pt...HC11c	2.53 (7)	Pt-C1-HC1b	113.3 (31)
Pt...HC11b	2.89 (5)	Ti-C1-HC1a	116.3 (32)
Ti-C1	2.115 (7)	Ti-C1-HC1b	121.1 (31)
Ti-C11	2.395 (8)	HC1a-C1-HC1b	109.0 (45)
Ti-CpA	2.081	Pt-C11-Ti	75.6 (2)
Ti-CpB	2.082	Pt-C11-HC11a	105.1 (42)
Ti...HC1a	2.67 (5)	Pt-C11-HC11c	103.7 (40)
Ti...HC1b	2.74 (5)	Pt-C11-HC11b	127.1 (28)
Ti...HC11b	1.93 (5)	Ti-C11-HC11b	51.7 (27)
Ti...HC11a	2.94 (6)	Ti-C11-HC11a	122.3 (42)
Ti...HC11c	3.07 (7)	Ti-C11-HC11c	126.3 (40)
C1...C1	3.348 (11)	HC11a-C11HC11b	101.2 (50)
P-C3	1.828 (9)	HC11b-C11-HC11c	109.3 (48)
P-C4	1.829 (9)	HC11c-C11-HC11a	109.9 (58)
P-C5	1.829 (6)	Pt-P-C3	112.4 (3)
C1-HC1a	0.94 (5)	Pt-P-C4	115.9 (3)
C1-HC1b	0.96 (5)	Pt-P-C5	119.0 (2)
C11-HC11a	0.85 (6)		
C11-HC11c	0.97 (7)		
C11-HC11b	1.06 (5)		

Structure of 2c. The Ti-Pt distance (2.962 (2) Å) is significantly longer than that in 2e, but it is still in the range where a weak Pt → Ti interaction is possible. The Pt-CH₂ distance (2.112 (17) Å) is slightly longer than that in 2e and is typical of a Pt-C single bond which is trans to a phosphine ligand.¹² The Pt-Me bond length (2.071 (15) Å) is comparable with that of *trans*-PtMeCl(PMePh₂)₂ (2.081 (6) Å).¹⁵ The Pt-Cl and Ti-Cl distances are similar to those of the Cl-bridged compounds.¹⁶

Reactions. With Tertiary Phosphines. The PMePh₂-coordinated complex 2d (0.15 M) in THF-*d*₈ was treated with PMePh₂ (2.5 equiv/2d) at -70 °C. The clear red solution rapidly turned

(15) Bennett, M. A.; Chee, H.-K.; Robertson, G. B. *Inorg. Chem.* **1979**, *18*, 1061.

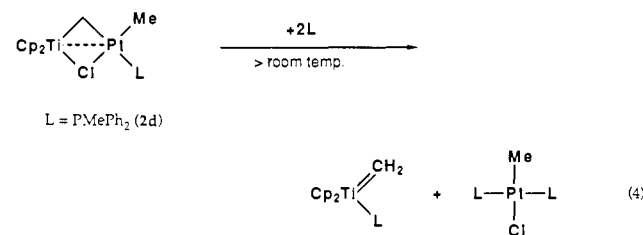
(16) (a) Parsons, E. J.; Larsen, R. D.; Jennings, P. W. *J. Am. Chem. Soc.* **1985**, *107*, 1793. (b) Whitla, W. A.; Powell, H. M.; Venanzi, L. M. *Chem. Commun.* **1966**, 310. (c) De Renzi, A.; Di Blassio, B.; Paiaro, G.; Panunzi, A.; Pedone, C. *Gazz. Chim. Ital.* **1976**, *106*, 765. (d) Struchkov, Yu. T.; Aleksandrov, G. G.; Pukhnarevich, V. B.; Sushchinskaya, S. P.; Voronkov, M. G. *J. Organomet. Chem.* **1979**, *172*, 269. (e) Goel, A. B.; Goel, S.; Vanderveer, D. *Inorg. Chim. Acta* **1981**, *54*, L267. (f) Olthof, G. J. *J. Organomet. Chem.* **1977**, *128*, 367. (g) Jungst, R.; Sekutowski, D.; Davis, J.; Luly, M.; Stucky, G. *Inorg. Chem.* **1977**, *16*, 1645. (h) van der Wal, H. R.; Overzet, F.; van Oven, H. O.; de Boer, J. L.; de Liefde Meijer, H. J.; Jellinek, F. J. *Organomet. Chem.* **1975**, *92*, 329. (i) Sekutowski, D.; Jungst, R.; Stucky, G. D. *Inorg. Chem.* **1978**, *17*, 1848.



dark red. ¹H, ¹³C, and ³¹P NMR spectra of the solution have revealed a rapid equilibrium between 2d and a new μ -methylene species with two PMe₂Ph ligands (3d): [3d]/[2d][PMePh₂] = 30 M⁻¹ at -60 °C. The NMR data of 3d are listed in Table V. The two sets of doublets with ¹⁹⁵Pt satellites in the ³¹P{¹H} NMR spectrum indicate that the platinum center has two PMePh₂ ligands in a *cis* orientation. The relatively small ¹J_{PP} values (1795 and 1979 Hz) are within the typical magnitude for *cis*-dialkylbis(tertiary phosphine)platinum(II) complexes.¹⁰ The μ -methylene protons and carbon are observed as a slightly broad doublet of doublets at δ 5.16 in the ¹H NMR spectrum and at δ 158.1 in the ¹³C NMR spectrum. The chemical shifts are considerably higher than those for 2d. The ¹J_{CH} value for the μ -CH₂ group (113 Hz) is comparable with that for a typical methylene group in an acyclic hydrocarbon.⁹ Treatment of the equilibrium mixture with dry HCl (1 equiv/Ti) at -50 °C results in the spontaneous conversion of 3d into the kinetic products, Cp₂TiMe(Cl) and *trans*-PtMeCl(PMePh₂)₂; 2d is fairly stable to HCl under these reaction conditions. These results are consistent with the structure of 3d not including either a metal-metal bond or an additional bridging ligand.^{17,18}

A remarkable temperature dependence of the equilibrium (3) has been observed. The *K*_{eq} values ([3d]/[2d][PMePh₂], M⁻¹) in toluene-*d*₈ are 7.9 (-50 °C), 2.4 (-30), 0.69 (-10), and 0.0 (25). On the basis of these equilibrium constants, thermodynamic parameters at 223 K are estimated as follows: $\Delta H = -7.1$ kcal/mol, $\Delta S = -28$ eu; $\Delta G = -0.92$ kcal/mol. The large negative entropy is in accord with a ligand association and the sterically crowded structure of 3d.

Above room temperature, on the other hand, the system irreversibly forms Cp₂Ti(=CH₂)PMePh₂¹⁹ and *trans*-PtMeCl(PMePh₂)₂ (eq 4). The titanocene methyldene species thus



formed instantly decomposes into a paramagnetic titanium species under the reaction conditions.

Complex 2c shows similar reaction patterns in a solution containing PMe₂Ph. Treatment of 2c with PMe₂Ph at -70 °C instantly gives Cp₂(Cl)TiCH₂PtMe(PMe₂Ph)₂ (3c), which is in rapid equilibrium with 2c: [3c]/[2c][PMe₂Ph] = 1.1 × 10³ M⁻¹ in THF-*d*₈ at -60 °C. The NMR data of 3c in Table V suggest a similar structure to 3d. The equilibrium mixture of 2c and 3c is much more sensitive to temperature than that of 2d and 3d and irreversibly affords Cp₂Ti(=CH₂)PMe₂Ph¹⁹ and *trans*-PtMeCl(PMe₂Ph)₂ even at -30 °C. The greater tendency of the PMe₂Ph system to form the phosphine-coordinated titanocene methyldene species, as compared with the PMePh₂ system, may be correlated with the strong affinity of titanocene species for basic and compact phosphines.¹⁹ Indeed, treatment of 2b with the more basic and compact PMe₃ rapidly gave Cp₂Ti(=CH₂)PMe₃ even

(17) The presence of Pt-Cl and/or Ti-Pt bond(s) makes the two μ -methylene hydrogens and the two Cp groups nonequivalent; it is inconsistent with the NMR results.

(18) There are two precedents of binuclear μ -methylene complexes without a metal-metal bond or an additional bridging ligand: Reference 6d. Arsenault, G. J.; Crespo, M.; Puddephatt, R. J. *Organometallics* **1987**, *6*, 2255.

(19) (a) Meinhart, J. D.; Anslin, E. V.; Park, J. W.; Grubbs, R. H., unpublished results. (b) Meinhart, J. D. Ph.D. Thesis, California Institute of Technology, Pasadena, CA, 1987.

Table V. NMR Data for the μ -Methylene (**3c**, **3d**) and μ -(C,O)-Ketene Complexes (**4c**, **4d**)^a

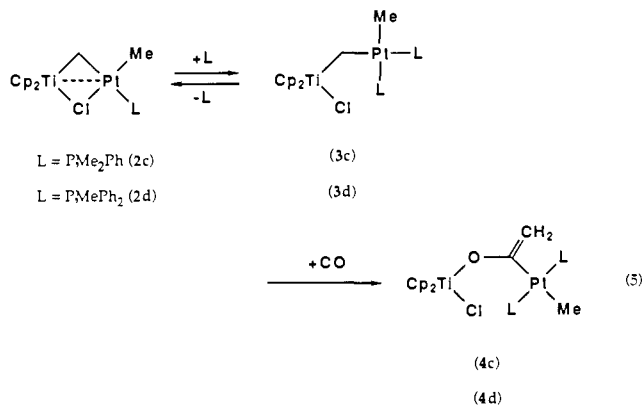
complex	¹ H NMR			¹³ C{ ¹ H} NMR			assignment	³¹ P{ ¹ H} NMR		
	δ	J, Hz		δ	J, Hz			δ^d	¹ J _{PtP} , Hz	
3c (THF- <i>d</i> ₈ , -60 °C)	6.18 (s)	0.0	0.0	114.7 (s)	0	0	175	Cp	-6.6 (d)	1841
	5.19 (dd)	7.9 ^a	68.1	158.4 (dd)	106, 10	670	114	μ -CH ₂	-15.3 (d)	1880
	1.40 (dd)	8.3	<i>b</i>	14.3 (dd)	29, 2	<i>b</i>	129	PMe	(² J _{PP} = 11 Hz)	
	1.21 (d)	7.8	<i>b</i>	14.2 (dd)	29, 2	<i>b</i>	129	PMe'		
	0.07 (dd)	9.3, 7.3	66.2	0.5 (dd)	103, 8	589	124	PtMe	(toluene- <i>d</i> ₈ , -50 °C)	
3d (THF- <i>d</i> ₈ , -60 °C)	6.08 (s)	0.0	0.0	114.5 (s)	0	0	174	Cp	10.0 (d)	1795
	5.16 (dd)	7.9 ^a	69.8	158.1 (dd)	108, ~8 ^b	674	113	μ -CH ₂	4.2 (d)	1979
	1.40 (d)	7.8	<i>b</i>	13.8 (d)	30	<i>b</i>	130	PMe	(² J _{PP} = 8 Hz)	
	1.36 (d)	7.6	<i>b</i>	13.2 (d)	32	<i>b</i>	131	PMe'		
	-0.12 (dd)	9.8, 7.3	64.9	3.7 (dd)	99, 8	600	126	PtMe		
4c (toluene- <i>d</i> ₈ , 25 °C)	5.99 (s)	0.0	0.0	207.9 (t)	11	683	<i>c</i>	C=CH ₂	-6.2 (s)	3015
	4.75 (s)	0.0	54.7	114.9 (s)	0	0	<i>c</i>	Cp		
	3.96 (s)	0.0	22.5					=CH		
				95.0 (s)	0	74	<i>c</i>	=CH ₂		
	1.66 (br t)	~3 ^b	32.7	13.2 (br t)	17	<i>b</i>	<i>c</i>	PMe		
4d (toluene- <i>d</i> ₈ , -20 °C)	0.05 (t)	6.8	48.8	-10.6 (t)	8	403	<i>c</i>	PtMe		
				207.8 (t)	10	664	<i>c</i>	C=CH ₂	9.2 (s)	3110
	5.77 (s)	0.0	0.0	115.0 (s)	0	0	<i>c</i>	Cp		
	4.66 (s)	0.0	53.7					=CH		
	4.00 (s)	0.0	20.8					=CH'		
			96.6 (s)	0	64	<i>c</i>	=CH ₂			
2.28 (br t)	~3 ^b	<i>b</i>	14.1 (t)	19	<i>b</i>	<i>c</i>	PMe			
-0.12 (t)	6.6	47.6	-6.5 (t)	7	403	<i>c</i>	PtMe			

^aThe signal appeared as a pseudotriplet. ^bCoupling constant is obscure due to broadening. ^cNot measured. ^dChemical shift is relative to an external 85% H₃PO₄ standard (downfield positive).

at -50 °C. In this system, formation of Cp₂(Cl)TiCH₂PtMe(PMe₃)₂ has also been suggested by NMR spectroscopy. Adequate identification of the μ -methylene complex could not be achieved due to its instability.

In contrast to the high reactivity of μ -Cl/ μ -CH₂ complexes, the μ -Me/ μ -CH₂ analogues **2e** and **2f** are significantly more stable toward tertiary phosphines. For example, complex **2e** is totally unreactive with PMe₂Ph below 0 °C, while it slowly forms Cp₂Ti(=CH₂)PMe₂Ph and the corresponding dimethylplatinum species at room temperature. The higher stability of the μ -Me complexes relative to the μ -Cl analogues may arise from the stronger Pt-Ti bond in the former complexes. The palladium complex **2g** rapidly reacts with PMe₃ at -50 °C to give *trans*-PdMeCl(PMe₃)₂ and a paramagnetic titanium species. In this system, formation of a small amount of Cp₂Ti(=CH₂)PMe₃ has also been noted.

With Carbon Monoxide. The μ -methylene complexes **3c** and **3d** exhibit significantly high reactivities toward CO insertion. An equilibrium mixture of **2c** and **3c** prepared from **2c** and an



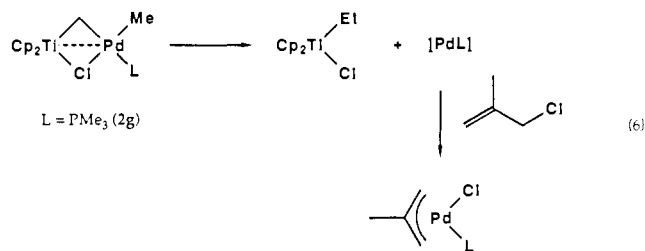
equimolar amount of PMe₂Ph in toluene-*d*₈ ([**3c**]/[**2c**] = 4) was treated at -70 °C with an excess amount of carbon monoxide. When the temperature was raised to -50 °C, the color of the system quickly changed from deep red to yellowish brown. NMR analysis of the reaction solution showed formation of the μ -(C,O)-ketene complex (**4c**) in 80% selectivity together with a small amount of *trans*-PtMeCl(PMe₂Ph)₂. Similarly, the reaction of

2d, PMePh₂, and CO gave the μ -(C,O)-ketene complex having PMePh₂ ligands (**4d**) in over 95% selectivity.

The ketene complexes are extremely moisture-sensitive, oily materials and could not be isolated in a pure state. NMR spectroscopy, however, gave unambiguous support to their structures (Table V). The chemical shifts of vinylic carbons and protons in the μ -ketene group are comparable with those for the Zr/Zr, Zr/Pt,²⁰ and Zr/Fe μ -(C,O)-ketene analogues.²¹ The triplet signals for PtMe and PMe protons and carbons indicate a *trans* configuration at the platinum center.

In the absence of added tertiary phosphines, complexes **2c** and **2d** under a CO atmosphere give Ti/Pt μ -methylene species with a CO ligand at the platinum center, Cp₂(Cl)TiCH₂PtMe(CO)L (see the Experimental Section). No sign of CO insertion, however, has been observed in these systems. Complexes **2e**, **2f**, and **2g** show little reactivity toward carbon monoxide.

Reductive Elimination Reaction. Among the μ -methylene complexes described above, the titanium/palladium complex **2g**



is thermally unstable in solution and above room temperature readily undergoes a reductive elimination reaction to give Cp₂Ti(Et)Cl and [Pd⁰PMe₃]. The latter species, formally a 12-electron complex, spontaneously decomposes under the reaction conditions to give metallic palladium and free PMe₃. The PMe₃ thus released successively attacks **2g** to form *trans*-PdMeCl(PMe₃)₂ and a paramagnetic titanium species. In the presence of 3-chloro-2-methylpropene, on the other hand, the Pd(0) species

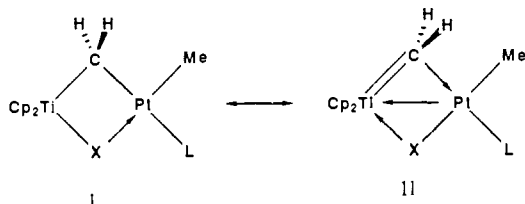
(20) (a) Ho, S. C. H.; Straus, D. A.; Armantrout, J.; Schaefer, W. P.; Grubbs, R. H. *J. Am. Chem. Soc.* **1984**, *106*, 2210. (b) Ho, S. C. H. Ph.D. Thesis, California Institute of Technology, Pasadena, CA, 1986.

(21) Weinstock, I.; Floriani, C.; Chiesi-Villa, A.; Guastini, C. *J. Am. Chem. Soc.* **1986**, *108*, 8298.

is effectively trapped as a stable π -allylpalladium chloride complex, and the reductive elimination reaction can be observed to proceed in over 80% selectivity. As reaction 6 proceeds, it obeys first-order kinetics regarding the concentration of **2g** up to 75% conversion. The reaction rate is only slightly dependent on the 3-chloro-2-methylpropene concentration. Further study of the mechanistic details, particularly of the effect of added tertiary phosphine on the reductive elimination reaction, could not be performed because of the extremely high reactivity of **2g** toward phosphines to afford mononuclear titanium species and monomethylpalladium chloride.

Discussion

The titanium/platinum μ -methylene complexes have two limiting descriptions of bonding, I and II. In structure I, the μ -



methylene carbon is linked to the metal centers with σ bonds. Structure II, on the other hand, consists of $\text{Cp}_2\text{Ti}=\text{CH}_2$ and $\text{PtMe}(\text{X})\text{L}$ moieties. The $\text{Ti}=\text{CH}_2$ group is bound to the platinum center in a π -bonding manner. The present results suggest that the proper bonding description lies somewhere between I and II, and the relative contribution of both structures varies with the bridging ligand X.

The contribution of structure II is reflected in the short $\text{Ti}-\text{CH}_2$ distances in **2c** and **2e**. The tilting of the CH_2 plane toward the platinum center, which indicates residual double-bonding character between Ti and the CH_2 group, is also consistent with bonding description II. In this structure the dative $\text{Pt} \rightarrow \text{Ti}$ interaction may be regarded as a π back-donation from an occupied d orbital on platinum to the π^* orbital of the "titanaolefin" group, which is localized on the electropositive titanium atom. Similar to the bonding of general transition-metal olefin complexes, the π back-donation will shorten the $\text{Ti}-\text{Pt}$ and $\text{Pt}-\text{CH}_2$ bonds and elongate the $\text{Ti}-\text{CH}_2$ distance. That is, the longer $\text{Ti}-\text{CH}_2$ bond and the shorter $\text{Ti}-\text{Pt}$ and $\text{Pt}-\text{CH}_2$ distances in **2e** than those in **2c** can be considered to reflect the higher contribution of II to **2e**. In complex **2e**, the μ -Me group is ligated to titanium with its C-H σ -bonding electrons and to platinum by a normal covalent bond. The greater π -acidic nature of titanium compared to that of platinum may be responsible for this bonding pattern and facilitates the contribution of II to **2e**.

The reaction in eq 3 strongly suggests the predominant contribution of structure I to the μ - CH_2/μ -Cl complexes. These compounds have two electrophilic metal centers with formal 16-electron configurations. Nucleophilic attack of phosphine at the platinum center induces cleavage of the $\text{Pt}-\text{Cl}$ bond to give **3c** and **3d**, which are in rapid equilibrium with **2c**:L and **2d**:L, respectively (Scheme I; path a). This reaction readily proceeds even at -70°C .

At elevated temperatures, on the other hand, this kinetically preferred reaction becomes unfavorable due to the large negative entropy arising from the sterically crowded structures of **3c** and **3d** and the less favorable attack of phosphine at the titanium center takes place (path b). This reaction affords the titanocene methylidene species, which may be weakly coordinated to the $[\text{PtMe}(\text{Cl})\text{L}]$ moiety. Successive attack by another phosphine at the platinum atom yields the monomethylplatinum and methylidenetitanium complexes. Reaction path b is consistent with a partial contribution by structure II to the μ - CH_2/μ -Cl complexes, in agreement with the X-ray structure of **2c**.

The μ -methylene complexes with $\text{Ti}-\text{Pt}$ bonds (**2a**–**2f**) show high stability toward CO insertion. In contrast, complexes **3c** and **3d** react rapidly with CO to give μ -(C,O)-ketene species **4c** and **4d**, respectively. The first step of this transformation is proposed to be CO insertion into the $\text{Ti}-\text{CH}_2$ bond to form a μ -(C,C)-ketene complex A (Scheme II).²²

As is well documented for mononuclear acyl complexes of group 4 metals,²³ a μ -(C,C)-ketene group ligated to titanium in an η^2 -coordination manner should have oxycarbene character (B). This will induce successive 1,2-migration of the $\text{PtMe}(\text{Cl})\text{L}$ group to form a μ -(C,O)-ketene complex.^{20,24}

Despite an abundance of μ -methylene complexes, there are currently only three definitive examples of carbonylation of a μ -methylene species to give a μ -ketene complex.⁶ Two of them are related to trinuclear osmium clusters,^{6b,c} and the other one is related to the binuclear ruthenium complex $[\text{Cp}(\text{CO})_2\text{Ru}]_2\text{CH}_2$.^{6d} The present reaction is analogous to the latter case except that the ruthenium system gives the μ -(C,C)-ketene species, while the present reaction gives the μ -(C,O)-ketene complex, owing to the highly oxophilic character of titanium. In the ruthenium complex the two Ru atoms are linked to each other only by the μ - CH_2 ligand, and there is neither an additional bridging group nor a metal-metal bond. The NMR data suggest that the present complexes **3c** and **3d** possess a similar bonding feature. The lack of additional bonding between the two metal centers in these μ -methylene complexes may be responsible for their much greater reactivity toward CO insertion, as compared with the corresponding μ -methylene complexes with metal-metal bonds.

The present study revealed several interesting bonding and reactivity features of the titanium/platinum and palladium μ -methylene complexes. These features have not been observed in other well-known late-transition-metal μ -methylene complexes.⁴ The presence of the two metal centers of significantly different properties, namely the electron-deficient titanium and the electron-rich platinum and palladium atoms, is responsible for these unique bonding and reactivity patterns. Similar patterns may occur in the early/late heterobimetallic catalysts in the SMSI state and serve as an important reason for their high activity in catalytic CO hydrogenation.

Experimental Section

¹H and ¹³C{¹H} NMR spectra were recorded on JEOL GX-400 (¹H, 399.8 MHz; ¹³C, 100.4 MHz) and FX-90Q (¹H, 89.6 MHz) spectrometers by using ¹H (of residual protons) and ¹³C NMR signals of deuterated solvents as internal references [benzene-*d*₆ (¹H, δ 7.15; ¹³C, δ 128.0), toluene-*d*₈ (¹H, δ 2.09; ¹³C, δ 20.4), THF-*d*₈ (¹H, δ 3.58; ¹³C, δ 67.4), CDCl₃ (¹H, δ 7.24)]. ¹J_{CH} values were determined by ¹³C NMR spectroscopy in an INEPT sequence. ³¹P{¹H} NMR signals were obtained on a JEOL FX-90Q spectrometer (36.2 MHz) and their chemical shifts referred to an external 85% H₃PO₄ standard (downfield positive). Infrared spectra were measured on a Perkin-Elmer 1720 (FT) spectrometer. Elemental analyses were performed by the California Institute of Technology Analytical Facility.

All manipulations were carried out under argon or vacuum with standard Schlenk techniques or in a nitrogen-filled glovebox. Argon was purified by passage through columns of Chemalog R3-11 catalyst and Linde 4-Å molecular sieves. Toluene, benzene, diethyl ether, pentane, and THF, including NMR solvents, were dried over sodium benzo-phenone ketyl and vacuum transferred and stored in flasks equipped with Teflon screw valves. Carbon monoxide (Matheson), tertiary phosphines (Strem), and an Et₂O solution of MeMgBr (Aldrich) were used as purchased. $[\text{PdMe}(\mu\text{-Cl})\text{PMe}_3]_2$ was prepared by a method similar to its PEt₃ analogue.²⁵ ¹H NMR (CDCl₃): δ 0.61 (d, *J*_{PH} = 2.4 Hz, 6 H, PdMe), 1.40 (d, *J*_{PH} = 11.0 Hz, 18 H, PME).

Preparation of 2c. To a toluene solution of **2a**^{5b} prepared from $\text{Cp}_2\text{TiCH}_2\text{C}(\text{Me})_2\text{CH}_2$ (1, 0.20 g, 0.82 mmol),¹³ $\text{PtMeCl}(\text{SMe}_2)_2$ (0.30 g, 0.82 mmol),²⁶ and toluene (3 mL) was added 116 μL of PMe_2Ph at

(22) An alternative process involving a CO insertion into the $\text{Pt}-\text{CH}_2$ bond is unlikely because *cis*-dialkylplatinum(II) complexes are known to possess great stability toward CO insertion: Booth, G.; Chatt, J. *J. Chem. Soc. A* **1966**, 634. In contrast, CO insertion into a $\text{Ti}-\text{R}$ bond to give a $\text{Cp}_2\text{Ti}(\text{COR})\text{Cl}$ complex proceeds under mild conditions: Fachinetti, G.; Floriani, C. *J. Organomet. Chem.* **1974**, 71, C5.

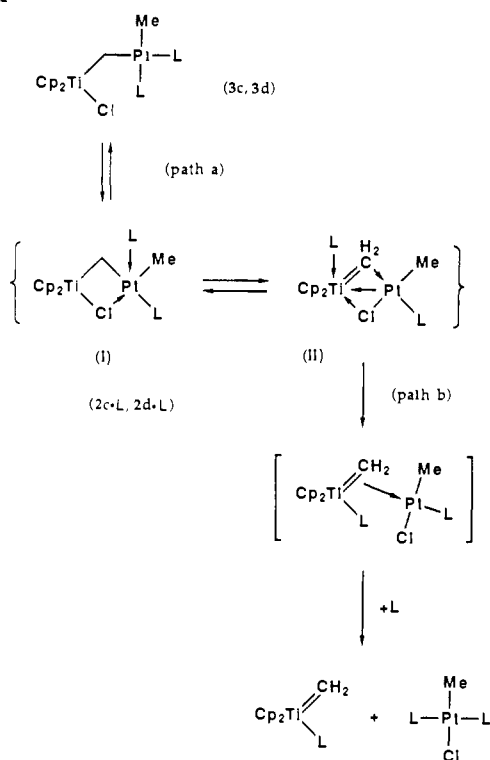
(23) (a) Wolczanski, P. T.; Bercaw, J. E. *Acc. Chem. Res.* **1980**, 13, 121. (b) Tatsumi, K.; Nakamura, A.; Hofmann, P.; Stanfert, P.; Hoffmann, R. *J. Am. Chem. Soc.* **1985**, 107, 4440, and references cited therein.

(24) Marquez, J. M.; Fagan, P. J.; Marks, T. J.; Day, C. S.; Day, V. W. *J. Am. Chem. Soc.* **1978**, 100, 7112.

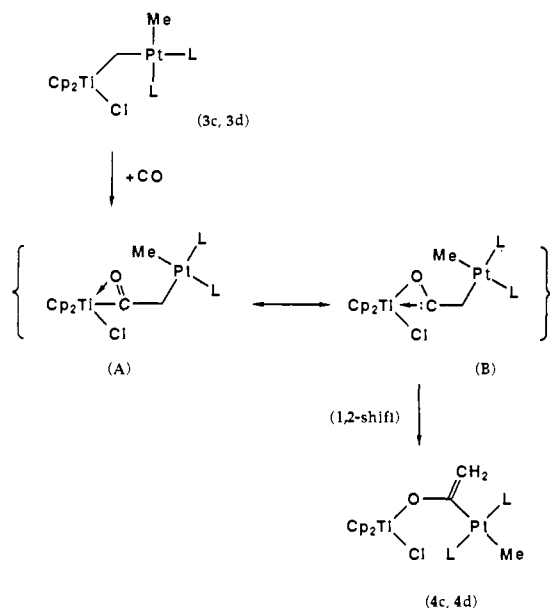
(25) Scott, J. D.; Puddephatt, R. *J. Organometallics* **1983**, 2, 1643.

(26) Hayashi, Y.; Isobe, K.; Nakamura, Y.; Okeya, S. *J. Organomet. Chem.* **1986**, 310, 127.

Scheme I



Scheme II



-20°C . After the solution was stirred for 2 h at room temperature, volatiles were removed under vacuum. The resulting red solid was dissolved in toluene (2 mL), diluted with pentane (4 mL), and then filtered through a filter-paper-tipped cannula. The filtrate was slowly cooled to -50°C to yield red crystals of **2c**, which were collected by filtration, washed with cold pentane (2 mL \times 2), and dried under vacuum (0.43 g, 92%). Anal. Calcd for $\text{C}_{20}\text{H}_{26}\text{ClPPtTi}$: C, 41.72; H, 4.55. Found: C, 41.56; H, 4.59. Similarly prepared was $\text{Cp}_2\text{Ti}(\text{CH}_2)\text{PtCl}(\text{Me})\text{PMePh}_2$ (**2d**) by using PMePh_2 in place of PMe_2Ph (52%). Anal. Calcd for $\text{C}_{25}\text{H}_{28}\text{ClPPtTi}$: C, 47.07; H, 4.42. Found: C, 47.19; H, 4.51. Reaction of **2a** and PMe_3 in toluene gave the PMe_3 analogue (**2b**) as a spectroscopically pure, red oil after removal of volatiles under reduced pressure.

Preparation of 2e. To a homogeneous solution of **2c** (0.70 g, 1.2 mmol) in a toluene (11 mL) and Et_2O (11 mL) mixture was added dropwise a Et_2O solution of MeMgBr (2.2 mL, 4.1 mmol) at room temperature. After it was stirred for 3 h, the mixture was concentrated to dryness under vacuum and extracted with toluene (22 mL). The extract was again concentrated to dryness to give a reddish orange solid, which was dissolved in Et_2O (30 mL) and cooled to -50°C to yield

crystals of **2e** (0.29 g, 42%). ^1H NMR analysis showed that the product contains 4% of the geometrical isomer **2f**, which could not be removed by repeated recrystallizations. Anal. Calcd for $\text{C}_{21}\text{H}_{29}\text{PPtTi}$: C, 45.41; H, 5.26. Found: C, 45.37; H, 5.07. IR (KBr): 2516 cm^{-1} (ν_{CH} of the agostic hydrogen).

Preparation of 2f. A solution of **2e** (0.20 g, 0.36 mmol) in toluene (3 mL) and Et_2O (3 mL) was combined with a Et_2O solution of MeMgBr (200 μL , 0.37 mmol) at room temperature. After the solution was stirred for 19 h, volatiles were removed under vacuum, and the resulting solid was extracted with toluene (4 mL). The extract was again concentrated to dryness to form a precipitate of **2f**. The crude product was recrystallized from Et_2O (5 mL) at -50°C to yield reddish orange crystals (0.13 g, 65%). ^1H NMR spectrum of the product revealed contamination with **2e** (4%) and an unidentified compound (6%), which could not be removed by repeated recrystallizations. Anal. Calcd for $\text{C}_{21}\text{H}_{29}\text{PPtTi}$: C, 45.41; H, 5.26. Found: C, 44.59; H, 5.05. IR (KBr): 2518 cm^{-1} (ν_{CH} of the agostic hydrogen).

Preparation of 2g. To a Schlenk flask containing the titanacyclobutane **1** (0.15 g, 0.60 mmol) and $[\text{PdMe}(\mu\text{-Cl})\text{PMe}_3]_2$ (0.14 g, 0.30 mmol) was added toluene (3 mL) at -20°C . The heterogeneous mixture was stirred at 0°C for 2 h and then at 10°C for 3 h to give a red solution containing a small amount of brown precipitate. The solution was filtered through a filter-paper-tipped cannula, diluted with pentane (5 mL), and cooled to -50°C . After 4 days, red crystals of **2g** formed. The product was washed with cold pentane (3 mL \times 2) and dried under vacuum at 0°C (0.16 g, 59%). The crystalline product contained 0.3 equiv/**2g** of toluene as confirmed by ^1H NMR spectroscopy. Anal. Calcd for $\text{C}_{15}\text{H}_{24}\text{ClPPdTi} \cdot 0.3\text{C}_7\text{H}_8$: C, 45.37; H, 5.88. Found: C, 45.37; H, 5.78.

Reactions of 2d and 2c with Tertiary Phosphines. A solution of **2d** (22.7 mg, 0.0356 mmol) in THF-d_8 (400 μL) was placed in an NMR sample tube equipped with a rubber septum cap. At -70°C , PMePh_2 (17 μL , 0.090 mmol) was added by means of a syringe. The clear red solution turned deep red within a few minutes. NMR analysis at -60°C revealed that the system contains **2d** and **3d** in a 18:82 ratio; the value is based on relative Cp peak integration. The characteristic NMR data for **3d** are listed in Table V.

The same reaction was examined over the temperature range -50 to $+25^\circ\text{C}$ by using **2d** (18.3 mg, 0.0289 mmol), PMePh_2 (7.4 μL , 0.039 mmol), and toluene- d_8 (400 μL) as the solvent. When the temperature was raised, the deep red solution turned clear red, and when it cooled, the system again exhibited the deep red color. This color change was accompanied by an alteration in a relative ratio of **2d** and **3d** as confirmed by ^1H NMR spectroscopy. The equilibrium constants ($K_{\text{eq}} = [\text{3d}]/[\text{2d}][\text{PMePh}_2]$) at four different temperatures and the thermodynamic parameters are given in the text. When the solution was allowed to stand at room temperature, gradual formation of $\text{Cp}_2\text{Ti}(\text{=CH}_2)\text{PMePh}_2^{19}$ and $\text{trans-PtMeCl}(\text{PMePh}_2)_2^{27}$ was observed over 24 h in the ^1H NMR spectra. Identification of these compounds was achieved by comparison with ^1H NMR spectra of authentic samples measured under similar conditions. ^1H NMR [$\text{Cp}_2\text{Ti}(\text{=CH}_2)\text{PMePh}_2$]: δ 12.39 (d, $J_{\text{PH}} = 6.3$ Hz, CH_2), 5.32 (d, $J_{\text{PH}} = 2.0$ Hz, Cp), 1.55 (d, $J_{\text{PH}} = 6.3$ Hz, PMe). ^1H NMR [$\text{trans-PtMeCl}(\text{PMePh}_2)_2$]: δ 0.27 (br, $J_{\text{PH}} = 79.1$ Hz, PtMe). The methylenide complex was unstable under the reaction conditions and readily decomposed into an unidentified paramagnetic titanium species.

The reaction of **2c** and PMe_2Ph was similarly examined. The NMR data for **3c** in THF-d_8 at -60°C are given in Table V. The system rapidly afforded $\text{Cp}_2\text{Ti}(\text{=CH}_2)\text{PMe}_2\text{Ph}^{19}$ and $\text{trans-PtMeCl}(\text{PMe}_2\text{Ph})_2^{27}$ above -30°C . The ^1H NMR data of these compounds in toluene- d_8 at -10°C are as follows. ^1H NMR [$\text{Cp}_2\text{Ti}(\text{=CH}_2)\text{PMe}_2\text{Ph}$]: δ 12.29 (d, $J_{\text{PH}} = 6.8$ Hz, CH_2), 5.34 (d, $J_{\text{PH}} = 2.4$ Hz, Cp), 1.09 (d, $J_{\text{PH}} = 5.9$ Hz, PMe). ^1H NMR [$\text{trans-PtMeCl}(\text{PMe}_2\text{Ph})_2$]: δ 1.39 (br, PMe), 0.38 (br, $J_{\text{PH}} = 80.5$ Hz, PtMe). These NMR data were in fair agreement with those of authentic samples measured under similar conditions.

Reaction of 3c and CO. To a solution of **2c** (21.6 mg, 0.375 mmol) in toluene- d_8 (0.4 mL) in an NMR sample tube equipped with a rubber septum cap was added PMe_2Ph (5.3 μL , 0.37 mmol) at -70°C . CO gas (1 atm) was then introduced by means of a syringe. When the temperature was raised to -50°C , the deep red color of the solution quickly changed to yellowish brown. After standing at -50°C for 12 h, the solution was examined by NMR spectroscopy. The ^1H NMR spectrum showed formation of **4c** (80%/2c) and $\text{trans-PtMeCl}(\text{PMe}_2\text{Ph})_2$ (20%); the yields are based on relative PtMe peak integration. Comparison of peak integrations of the Cp and PMe signals suggested that ca. 20% of titanium is converted into a paramagnetic species. The NMR data for **4c** are listed in Table V. The same reaction was performed in a Schlenk flask. After completion of the reaction, the volatile products were removed under vacuum to give a brown, oily material. NMR analysis of this product showed formation of **4c** in a selectivity similar to the NMR

tube reaction. Several attempts to obtain **4c** as a pure compound were unsuccessful.

Reaction of 3d and CO. An NMR sample tube containing **2d** (17.7 mg, 0.0278 mmol) and PMePh_2 (5.6 μL , 0.030 mmol) was attached to a vacuum line, and toluene- d_8 (0.4 mL) stored over sodium benzophenone ketyl was introduced by vacuum transfer at -196°C . The system was warmed to -78°C , and CO gas (1 atm) was then introduced. After the tube as sealed, the system was allowed to stand at -20°C for 3 days. NMR analysis of the resulting solution revealed formation of **4d** in 95% selectivity together with a small amount of *trans*- $\text{PtMeCl}(\text{PMePh}_2)_2$. The NMR data of **4d** are given in Table V.

Reaction of 2d and CO in the Absence of PMePh_2 . A solution of **2d** (16.7 mg, 0.0262 mmol) in toluene- d_8 (0.4 mL) was placed in an NMR sample tube. After the system was evacuated, CO gas (1 atm) was introduced at -78°C . The sample tube was sealed with a flame and allowed to stand at -50°C for 6 h. The clear red color of the solution turned reddish purple. NMR analysis of the solution revealed that the system contains **2d** and a new μ -methylene complex **5d** in a 4:21 ratio. The NMR data for **5d** (toluene- d_8 , -30°C) are as follows. ^1H NMR: δ 6.11 (d, $J_{\text{PH}} = 6.1$ Hz, $J_{\text{PH}} = 61.5$ Hz, 2 H, $\mu\text{-CH}_2$), 5.93 (s, 10 H, Cp), 1.84 (d, $J_{\text{PH}} = 9.3$ Hz, $J_{\text{PH}} = 23.4$ Hz, 3 H, PMe), 1.03 (d, $J_{\text{PH}} = 10.7$ Hz, $J_{\text{PH}} = 68.4$ Hz, 3 H, PtMe). $^{31}\text{P}\{^1\text{H}\}$ NMR: δ 2.0 (s, $J_{\text{PP}} = 1911$ Hz). The same reaction was examined by using ^{13}C O (99.7% isotopic purity). In the ^1H NMR the PtMe and $\mu\text{-CH}_2$ protons showed a coupling toward the ^{13}C O: $J_{^{13}\text{CCH}_3} = 2.2$ Hz; $J_{^{13}\text{CCH}_2} = 2.9$ Hz. $^{13}\text{C}\{^1\text{H}\}$ NMR spectrum of the same solution exhibited a doublet signal assignable to a terminal ^{13}C O ligand coordinated to the platinum: δ 182.4 (d, $J_{\text{PC}} = 7$ Hz, $J_{\text{PC}} = 1092$ Hz). The coupling between the terminal ^{13}C O carbon and the phosphorus was observed also in the $^{31}\text{P}\{^1\text{H}\}$ NMR spectrum. These NMR data strongly suggest the structure $\text{Cp}_2(\text{Cl})\text{-TiCH}_2\text{PtMe}(\text{CO})\text{PMePh}_2$ for **5d**. The NMR sample solution was warmed to room temperature, and the reddish purple solution turned red. ^1H NMR spectrum of the solution showed reformation of **2d** at the cost of **5d** (**2d**:**5d** = 4:1 after 2 h at room temperature). In this spectrum several singlet peaks were also observed in the Cp region. After 1 day at room temperature, a ^1H NMR spectrum of this solution became complicated. No sign of CO insertion was observed.

Reaction of 2c (16.5 mg, 0.0286 mmol) and CO (1 atm) in toluene- d_8 (0.4 mL) was similarly examined. The reaction formed a μ -methylene complex **5c, a compound isostructural to **5d** (**2c**:**5c** = 1:9 at -50°C). ^1H NMR (-50°C): δ 6.18 (d, $J_{\text{PH}} = 6.1$ Hz, $J_{\text{PH}} = 59.1$ Hz, 2 H, $\mu\text{-CH}_2$), 5.93 (s, 10 H, Cp), 1.31 (d, $J_{\text{PH}} = 9.3$ Hz, $J_{\text{PH}} = 23.9$ Hz, 6 H, PMe), 1.04 (d, $J_{\text{PH}} = 10.7$ Hz, $J_{\text{PH}} = 68.4$ Hz, 3 H, PtMe); $J_{^{13}\text{CCH}_2} = 2.7$ Hz, $J_{^{13}\text{CCH}_3} = 2.4$ Hz. $^{13}\text{C}\{^1\text{H}\}$ NMR (-50°C , terminal CO only): δ 182.5 (d, $J_{\text{PC}} = 7$ Hz, $J_{\text{PC}} = 1092$ Hz). $^{31}\text{P}\{^1\text{H}\}$ NMR (-50°C): δ -14.0 ($J_{\text{PP}} = 1914$ Hz). At room temperature the system reproduced **2c** and formed some unidentified species. No sign of CO insertion, however, was observed.**

Reductive Elimination of 2g. A solution of **2g** (8.7 mg, 0.0250 mmol) in C_6D_6 (400 μL) was placed in an NMR sample tube equipped with a rubber septum cap, and 10 μL of 3-chloro-2-methylpropene (0.10 mmol) was added at room temperature. The tube was placed in an NMR sample probe controlled to $50.0 \pm 0.1^\circ\text{C}$. The reaction progress was followed by measurement of the change in relative Cp peak integration of **2g** and Cp_2TiEtCl in the ^1H NMR spectra. ^1H NMR spectrum at 100% conversion of **2g** showed formation of $\text{Cp}_2\text{TiEtCl}^{28}$ and $(\eta^3\text{-2-methylallyl})\text{Pd}(\text{Cl})\text{PMe}_3$ in 82% selectivity. ^1H NMR [Cp_2TiEtCl]: δ 5.78 (s, 10 H, Cp), 1.62 ($J_{\text{HH}} = 7.3$ Hz, 2 H, TiCH_2CH_3), 1.28 (t, $J_{\text{HH}} = 7.3$ Hz, 3 H, TiCH_2CH_3). ^1H NMR [$(\eta^3\text{-2-methylallyl})\text{Pd}(\text{Cl})\text{PMe}_3$]: δ 4.24 (d, $J_{\text{PH}} = 5.6$ Hz, 1 H, allyl H), 3.20 (d, $J_{\text{PH}} = 10.3$ Hz, 1 H, allyl H), 2.65 (br s, 1 H, allyl H), 2.02 (br s, 1 H, allyl H), 1.46 (s, 3 H, allyl Me), 0.99 (d, $J_{\text{PH}} = 9.8$ Hz, 9 H, PMe).²⁹ The reductive elimination rate constants ($10^4 k_{\text{obsd}}$, s^{-1}) at three different concentrations of 3-chloro-2-methylpropene (M) are as follows (at 50°C in C_6D_6 ; concentration of the chloride is in parentheses): 6.4 (0.51), 5.9 (0.25), 5.9 (0.13).

X-ray Diffraction Study of 2c. An irregular plate obtained by slow cooling of a Et_2O solution of **2c** was mounted in a capillary and placed on a CAD-4 diffractometer. Unit cell dimensions plus an orientation matrix were obtained from the setting angles of 25 reflections with $15^\circ < 2\theta < 21^\circ$. The cell dimensions suggested a monoclinic cell, and systematic absences in the diffractometer data indicated the space group $P2_1/n$, an unconventional setting of $P2_1/c$. Data were collected at a scan rate of $2^\circ/\text{min}$, with 3 reflections monitored every 10000 s of X-ray exposure. These indicated a small linear crystal decay; the data were

corrected for this and for absorption. Lorentz and polarization factors were applied, and the data were placed on an approximately absolute scale by Wilson's method. The platinum position was easily found from a Patterson map and subsequent structure factor-Fourier cycles showed the remaining non-hydrogen atoms. After six cycles of least squares, hydrogen atoms were introduced at calculated positions on the benzene and cyclopentadienyl rings and at positions determined from difference maps for the methyl and methylene hydrogen atoms. Further refinement of the positional and anisotropic thermal parameters of the non-hydrogen atoms and the positional parameters of the bridging methylene group hydrogen atoms (the remaining hydrogen atoms being repositioned once) converged, with no shift greater than 0.03σ . The R index for reflections with $F_o^2 > 3\sigma(F_o^2)$ was 0.035.

X-ray Diffraction Study of 2e. A single crystal prepared by slow cooling of a Et_2O solution of **2e** was mounted in a greased capillary and centered on the diffractometer. Unit cell parameters and an orientation matrix were obtained by a least-squares calculation from the setting angles of 23 reflections with $42^\circ < 2\theta < 46^\circ$. Two equivalent data sets out to a 2θ of 50° were collected at scan rates varying between 2 and $4^\circ/\text{min}$ with three reflections monitored every 10000 s of X-ray exposure. The data were corrected for absorption and a slight decay. Lorentz and polarization factors were applied, and the two data sets were then merged to yield the final data set. Several visible cracks in the crystal parallel to the 100 planes did not noticeably affect the scan profiles. Systematic absences in the diffractometer data led to the choice of space group $P2_1/n$. Starting non-hydrogen atom positions were assumed from the results of **2c**. Hydrogen atom positions were determined by calculation (for benzene and cyclopentadienyl rings) or from difference maps (for the methyl and methylene groups). The three hydrogen atoms of the terminal methyl group bonded to the platinum atom were modeled by six evenly spaced half-population hydrogen atoms at calculated positions with isotropic B values 10% greater than that of the attached carbon; these were not refined. The complete least-squares full matrix, consisting of spatial and isotropic thermal parameters for the remaining hydrogen atoms, spatial and anisotropic thermal parameters for the non-hydrogen atoms, a scale factor, and a secondary extinction coefficient, contained 322 parameters. The hydrogen results were quite acceptable. A final difference Fourier showed deviations of less than $1 \text{ e } \text{\AA}^{-3}$, mostly attributable to absorption ripple near the two heavy atoms. The final R index was 0.0394 (0.0242 for $F_o^2 > 3\sigma(F_o^2)$) with a goodness of fit of 1.12.

Calculations were performed with programs of the CRYM Crystallographic Computing System and ORTEP. Scattering factors and corrections for anomalous scattering were taken from a standard reference.³⁰ $R = \sum |F_o - |F_c|| / \sum F_o$, for only $F_o^2 > 0$, and goodness of fit = $[\sum w(F_o^2 - F_c^2)^2 / (n - p)]^{1/2}$ where n is the number of data and p the number of parameters refined. The function minimized in least squares was $\sum w(F_o^2 - F_c^2)^2$, where $w = 1/\sigma^2(F_o^2)$. Variances of the individual reflections were assigned on the basis of counting statistics plus an additional term, $0.014I^2$. Variances of the merged reflections were determined by standard propagation of error plus another additional term, $0.014(I)^2$. The absorption correction was done by Gaussian integration over an $8 \times 8 \times 8$ grid. Transmission factors varied from 0.438 to 0.716 for **2c** and from 0.317 to 0.409 for **2e**. The secondary extinction parameters³¹ refined to 0.039 (10) $\times 10^{-6}$ (for **2c**) and 0.0477 (10) $\times 10^{-6}$ (for **2e**).

Acknowledgment. We acknowledge the financial support of the Department of Energy and the National Science Foundation. We thank the NSF for Grant CHE-821939 to purchase the diffractometer and the Exxon Educational Foundation for financial support.

Registry No. 1, 80122-07-2; **2a**, 117119-20-7; **2b**, 118204-82-3; **2c**, 118102-09-3; **2d**, 118102-10-6; **2e**, 118102-00-4; **2f**, 118141-32-5; **2g**, 118102-01-5; **3c**, 118102-03-7; **3d**, 118102-04-8; **4c**, 118102-06-0; **4d**, 118102-07-1; **5c**, 118102-12-8; **5d**, 118102-11-7; $\text{PtMeCl}(\text{SMe}_2)_2$, 87145-39-9; $[\text{PdMe}(\mu\text{-Cl})\text{PMe}_3]_2$, 118102-02-6; $\text{Cp}_2\text{Ti}(\text{=CH}_2)\text{PMePh}_2$, 118102-05-9; *trans*- $\text{PtMeCl}(\text{PMePh}_2)_2$, 24833-61-2; $\text{Cp}_2\text{Ti}(\text{=CH}_2)\text{-PMe}_2\text{Ph}$, 108969-89-7; *trans*- $\text{PtMeCl}(\text{PMe}_2\text{Ph})_2$, 24833-58-7; Cp_2TiEtCl , 12295-16-8; $(\eta^3\text{-2-methylallyl})\text{Pd}(\text{Cl})\text{PMe}_3$, 118102-08-2; 3-chloro-2-methylpropene, 563-47-3.

Supplementary Material Available: Atomic numbering schemes and tables of anisotropic displacement parameters, hydrogen parameters, and complete distances and angles (14 pages); tables of observed and calculated structure factors (24 pages). Ordering information is given on any current masthead page.

(28) Waters, J. A.; Mortimer, G. A. *J. Organomet. Chem.* **1970**, *22*, 417.
(29) These NMR data were in fair agreement with those of an authentic sample prepared from $[(\eta^3\text{-2-methylallyl})\text{Pd}(\mu\text{-Cl})]_2$ and PMe_3 : Dent, W. T.; Long, R.; Wilkinson, A. J. *J. Chem. Soc.* **1964**, 1585.

(30) Cromer, D. T.; Waber, J. T. *International Tables for X-ray Crystallography*; Kynoch Press: Birmingham, U.K., 1974; Vol. IV, pp 71 and 149.
(31) Equation 3 in: Larson, E. C. *Acta Crystallogr.* **1967**, *23*, 664.